

Modeling and open-loop control of IPMC actuators under changing ambient temperature

This article has been downloaded from IOPscience. Please scroll down to see the full text article.

2012 Smart Mater. Struct. 21 065014

(<http://iopscience.iop.org/0964-1726/21/6/065014>)

View [the table of contents for this issue](#), or go to the [journal homepage](#) for more

Download details:

IP Address: 23.28.250.20

The article was downloaded on 23/05/2012 at 02:38

Please note that [terms and conditions apply](#).

Modeling and open-loop control of IPMC actuators under changing ambient temperature

Roy Dong and Xiaobo Tan¹

Smart Microsystems Laboratory, Department of Electrical and Computer Engineering,
Michigan State University, East Lansing, MI 48824, USA

E-mail: dongroy@msu.edu and xbtan@msu.edu

Received 5 January 2012, in final form 27 March 2012

Published 22 May 2012

Online at stacks.iop.org/SMS/21/065014

Abstract

Because of the cost and complexity associated with sensory feedback, open-loop control of ionic polymer–metal composite (IPMC) actuators is of interest in many biomedical and robotic applications. However, the performance of an open-loop controller is sensitive to the change in IPMC dynamics, which is influenced heavily by ambient environmental conditions including the temperature. In this paper we propose a novel approach to the modeling and open-loop control of temperature-dependent IPMC actuation dynamics. An IPMC actuator is modeled empirically with a transfer function, the zeros and poles of which are functions of the temperature. With auxiliary temperature measurement, open-loop control is realized by inverting the model at the current ambient temperature. We use a stable but noncausal algorithm to deal with non-minimum-phase zeros in the system that would prevent directly inverting the dynamics. Experimental results are presented to show the effectiveness of the proposed approach in open-loop tracking control of IPMC actuators.

(Some figures may appear in colour only in the online journal)

1. Introduction

Ionic polymer–metal composites (IPMCs) are a class of soft actuation and sensing materials that has received significant interest over the past two decades [1]. An IPMC consists of three layers, with an ion ion-exchange polymer membrane (e.g. Nafion) sandwiched by metal or other conducting electrodes [2–4]. Inside the polymer, anions covalently fixed to polymer chains are balanced by mobile cations. An applied voltage across an IPMC leads to the transport of cations and accompanying solvent molecules, resulting in both differential swelling and electrostatic forces inside the material, which cause the material to bend and hence the actuation effect [1, 5, 6]. Conversely, an applied mechanical stimulus redistributes the cations inside an IPMC, producing a detectable electrical signal (typically open-circuit voltage or short-circuit current) that is correlated with the mechanical

stimulus, which explains the sensing mechanism of IPMCs [5, 7, 8]. IPMC materials have been proposed for various applications in actuation [9–16], sensing [17–24] and energy harvesting [25].

Control of IPMC actuators has received a great deal of attention over the years. Proposed control methods have spanned lead–lag compensation [26], PI or PID control [27–29], linear quadratic regulator (LQR) [30], adaptive control [31–34], H_∞ control [6] and impedance control [27]. These studies have mostly dealt with feedback control using bulky, external sensors, such as laser vibrometers [30, 31], laser distance sensors [6, 26–28, 33, 34], cameras [29] and load cells [26]. Because of size and safety concerns, it is unrealistic to adopt such large sensors in most envisioned micro-, bio- and robotic applications. This has motivated a number of groups to investigate compact integrated sensing schemes, including exploiting the correlation between surface resistance and bending curvature for position sensing [35–37], using a mechanically

¹ Author to whom any correspondence should be addressed.

coupled but electrically isolated IPMC sensor [29, 38–40], embedding a miniaturized strain gauge [41] and integrating polyvinylidene fluoride (PVDF) sensors [42, 43]. While these approaches hold promise in some applications, they increase the complexity and cost in the devices and processing circuits, especially for applications involving multiple IPMC actuators working in parallel. Therefore, it is often desirable to realize open-loop control of IPMC actuators, where the measurement of force or displacement output is not needed.

The performance of open-loop control depends on the availability of a precise model for IPMC actuators. However, IPMC dynamics could vary greatly, depending on the ambient environmental conditions, an important factor of which is the temperature. Among other things, the temperature could influence both ion transport dynamics and mechanical properties of the materials. There has been extensive work on modeling of IPMC actuators, from simple, empirical black-box models [26, 44], to gray-box models incorporating some level of material physics [45–47], to physics-based white-box models [5, 6, 48–56]. However, there have been very few studies, if any, on modeling of the temperature-dependent actuation dynamics of IPMCs. While the temperature variable often appears explicitly in physics-based models (e.g. [5]), these models do not fully capture all the important effects the temperature has on the material properties, examples of which include ionic diffusivity, Young's modulus, resistivity and dielectric permittivity. Recently, Ganley *et al* presented an empirical method for modeling temperature-dependent sensing behavior of IPMCs [57], which has motivated us to carry out a parallel study on the modeling of IPMC actuators.

In this paper we first present an approach to the modeling of temperature-dependent IPMC actuation dynamics. Since it is intractable to capture all effects of temperature using first principles, we adopt an empirical model taking the form of a transfer function. Each pole and zero of the transfer function is assumed to depend nonlinearly on the temperature. This nonlinear dependence is approximated with polynomial functions, the coefficients of which are identified through fitting of the poles/zeros obtained at a finite number of temperatures.

Second, we propose an inversion-based open-loop control strategy for IPMC actuators, where the aforementioned dynamic model evaluated at a given temperature is used. Note that this strategy assumes the availability of a temperature sensor for providing infrequent, auxiliary measurement of the temperature, which is not a stringent requirement in practice. The challenge, however, is that the obtained model for IPMC actuators is of non-minimum phase (zeros in the right half-plane) and its direct inverse would be unstable and thus not implementable. To address this, we apply a stable but noncausal inversion algorithm, which requires knowing the desired trajectories in advance. We further discuss a variant of the algorithm that only requires a finite-time preview of future trajectories to facilitate the practical use of the proposed control scheme. Experimental results are presented to illustrate and support the modeling and control methods.

The rest of the paper is organized as follows. The approach to the characterization and modeling of temperature-dependent IPMC dynamics, including the experimental

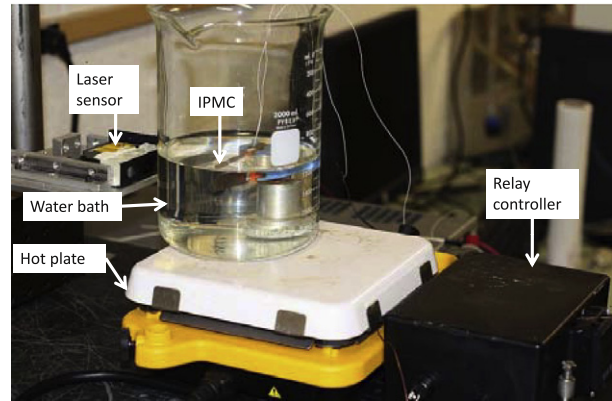
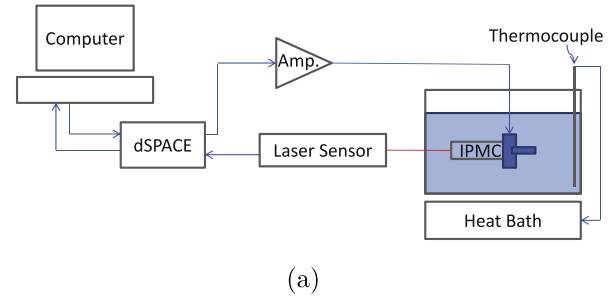


Figure 1. The experimental set-up for characterizing the temperature-dependent IPMC dynamics: (a) schematic and (b) actual set-up.

set-up, is presented in section 2. As we will see, the model consistently yields a non-minimum-phase transfer function at all temperatures in the experimental range. In section 3, we describe the inversion-based open-loop control scheme and present the experimental results on open-loop tracking. The implementation of the inverse compensation algorithm with finite-time preview is briefly discussed in section 4. Finally, we provide concluding remarks in section 5.

2. Modeling of temperature-dependent IPMC actuation dynamics

2.1. Experimental set-up

An IPMC sample, obtained from Environmental Robots Inc., was immersed in a temperature-controlled water bath to investigate its free-bending actuation performance under different temperatures. The experimental set-up is shown in figure 1. The IPMC beam was clamped at one end and was 0.3 mm thick and 11 mm wide, with a free length of 45 mm. The water bath was placed on a hotplate that was regulated by a relay controller (Auber Instruments, SYL-2342). A T-type thermocouple (Omega, HTTC36-T-116G-6) was used to measure the bath temperature and provide feedback for the relay controller. With this set-up, the temperature of the bath could be regulated with a precision of 0.5 °C. The actuation voltage signals were generated with dSPACE (dSPACE, DS1104) and applied to the IPMC beam. The

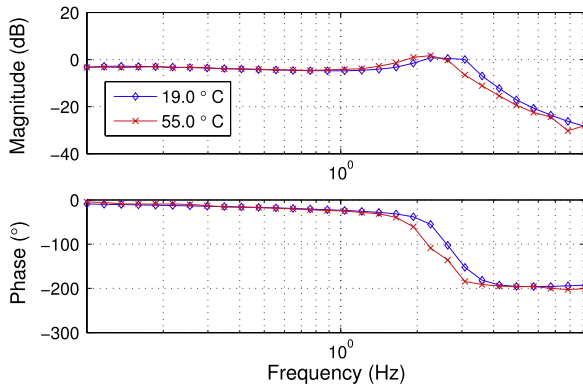


Figure 2. The measured frequency responses of the IPMC at two different temperatures, 19.0 and 55.0 °C. The output is tip displacement in mm and the input is applied voltage in V. The top plot shows the magnitude of the frequency response in dB; the bottom plot shows the phase of the frequency response in radians.

affected tip displacement of the IPMC was measured using a laser sensor (Baumer Electric, OADM 20I5441/S14F). Data acquisition was also done with dSPACE.

2.2. Characterization of temperature dependence

We characterized the dependence of IPMC actuation dynamics on temperature by measuring the empirical frequency responses at different temperatures, where the actuation voltage was taken as the input and the tip displacement (in millimeters) as the output. For a given temperature, 30 sinusoidal excitation signals with amplitude of 1 V were applied to the IPMC and the frequencies of these signals were logarithmically spaced between 0.1 Hz and 9 Hz. Because of the relatively low bandwidth of IPMCs, the IPMC would produce very little displacement for a higher frequency. For each frequency, a fast Fourier transform was performed on the input and the output signals to extract their amplitudes and phases. The empirical frequency response consisted of the amplitude gain (magnitude) and the phase shift between the input and the output at the tested frequencies.

The above procedure was performed for 10 different temperatures: 19.0, 21.5, 23.3, 25.0, 30.0, 35.0, 40.0, 45.0, 50.0 and 55.0 °C. At a given temperature, the sample was allowed to sit in the bath for sufficiently long time (over 20 min) before data collection was started, to ensure that the thermal effect had reached a steady state.

The collected empirical frequency response showed clear dependence on temperature. Figure 2 shows the frequency responses under 19.0 °C and 55.0 °C, the two extremes of the temperature used in the experiments. From the figure, among other things, as the temperature rises, the resonant frequency of the response shifts lower. The implication of the latter observation is significant, since an IPMC actuator is often operated around the resonant frequency to achieve the most effective actuation. In figure 2, the largest magnitude difference, occurring at about 3 Hz, is about 7 dB; in other words, at that frequency, the tip displacement of the IPMC actuator at 19.0 °C is more than twice that at 55.0 °C.

There are a number of factors that could contribute to the dependence of IPMC actuation behavior on temperature. For example, temperature has direct impact on the ion diffusion dynamics and could strongly affect the electrical properties (permittivity, resistivity), mechanical properties (Young's modulus) and the electromechanical coupling property. Attempting to quantify all these effects on a physics-based model is a formidable task and outside the scope of this paper. Instead, an empirical, black-box-type approach is taken to efficiently capture the temperature-dependent IPMC dynamics.

2.3. Temperature-dependent dynamic model

For a given temperature, the dynamics of the IPMC actuator is modeled as a linear time-invariant system represented by a transfer function

$$G(s) = \frac{b_m s^m + b_{m-1} s^{m-1} + \dots + b_1 s + b_0}{s^n + a_{n-1} s^{n-1} + \dots + a_1 s + a_0}. \quad (1)$$

Judging from the low-frequency phase response (close to 0°) in figure 2, we determine that the system is proper, which implies $m \leq n$ in (1). The inverse of a strictly proper system ($m < n$) would be improper and contain pure derivative terms, which could be problematic in implementing inverse-based open-loop control. For this reason, we will seek models where $m = n$. We assume that each of the coefficients $\{a_i\}_{i=0}^{n-1}$ and $\{b_i\}_{i=0}^n$ in (1) (or, equivalently, each pole and zero) depends nonlinearly on the temperature T and will approximate such nonlinear relationships with low-degree (such as quadratic) polynomial functions. The coefficients of the latter polynomial functions will be found by fitting the identified system poles and zeros at a finite set of test temperatures. The model is then used to predict the dynamics at any given temperature. We further elaborate this procedure below.

For a particular test temperature, we found transfer function models in the form of (1) with $m = n$ to fit the empirical frequency response, using the Matlab command `invfreqs`. In order to find a model with lowest complexity, we started with $n = 2$ (second-order) and moved upwards. It turns out that a second-order system failed to provide a good fit and had a relatively large magnitude error for each temperature. A third-order system provided a much better fit over a second-order system, but a fourth- or higher-order system provided little improvement over a third-order system. In particular, we found that using a fourth-order system would often result in a very large negative pole. For example, at 19 °C, the poles were found to be: -3.3874×10^9 , $-3.0168 \pm j16.8311$ and -2.3310 . The large magnitude of the first pole implies that it would have negligible effect compared to the other poles, and thus the fourth-order system can be effectively approximated with a third-order one. Based on these observations, we finally adopted a third-order model in the following form:

$$G(s) = \frac{b_3 s^3 + b_2 s^2 + b_1 s + b_0}{s^3 + a_2 s^2 + a_1 s + a_0}. \quad (2)$$

We also noticed that a strictly proper third-order system did not provide an improved fit over a system of the form (2), indicating no loss of model-fitting performance from enforcing a proper, but not strictly proper, model structure. Note that, while in principle an infinite-dimensional model is needed to fully describe the actuation physics of IPMCs [6], for a black-box modeling approach like that adopted in this paper, the measured frequency response within a finite frequency range can often be adequately captured by a low-order model.

We then converted the transfer function model identified for each temperature into a zero-pole form:

$$G(s) = k \frac{(s - z_1)(s - z_2)(s - z_3)}{(s - p_1)(s - p_2)(s - p_3)}, \quad (3)$$

where the seven parameters, $\{k, z_1, z_2, z_3, p_1, p_2, p_3\}$, characterize the model at any given temperature. For each parameter, we identified a quadratic function to approximate its dependence on temperature by fitting the parameter values at different temperatures. We illustrate the process by taking the example of obtaining $k(T) = c_2 T^2 + c_1 T + c_0$, where c_0 , c_1 and c_2 are the coefficients to be determined. Suppose that the identified parameter $k = \hat{k}_i$ at temperature T_i , $1 \leq i \leq N$. The coefficients c_0 , c_1 and c_2 are found using the least-squares approach, where

$$\sum_{i=1}^N (\hat{k}_i - k(T_i))^2 = \sum_{i=1}^N (\hat{k}_i - (c_2 T_i^2 + c_1 T_i + c_0))^2$$

is minimized. We used the Matlab command *polyfit* to solve the minimization problem. For identification of the quadratic functions for all seven parameters, we used 8 of the 10 tested temperatures ($N = 8$). We intentionally left out the data at two temperatures, 35.0 and 45.0 °C, so that they could be used for validation of the approach. Note that an alternative way of obtaining a temperature-dependent model is to fit each coefficient in (2) with a polynomial function of temperature. However, it was found that the coefficients of empirically fitted transfer functions showed a less consistent trend in their temperature dependence. This is because, for the same empirical response, it is possible to find multiple transfer function models that result in a similar level of approximation error.

For the IPMC sample used in this work, the fitted quadratic functions of temperature T were

$$k(T) = -3.7535 \times 10^{-5} T^2 + 0.0018T + 0.0381, \quad (4)$$

$$z_{1,2}(T) = (0.0217T^2 - 1.2721T + 33.6431) \quad (5)$$

$$\pm j(0.0238T^2 - 1.4177T + 64.0602), \quad (6)$$

$$z_3(T) = -8.7790 \times 10^{-4} T^2 + 0.0617T - 4.6059, \quad (7)$$

$$p_{1,2}(T) = (1.4314 \times 10^{-4} T^2 - 0.0039T - 2.9336) \quad (8)$$

$$\pm j(-6.1459 \times 10^{-4} T^2 - 0.0308T + 17.6483), \quad (8)$$

$$p_3(T) = -1.1396 \times 10^{-4} T^2 - 0.0141T - 2.1831. \quad (9)$$

As an example, figures 3(a) and (b) show the dependence of z_1 and p_1 on the temperature, respectively. Note that,

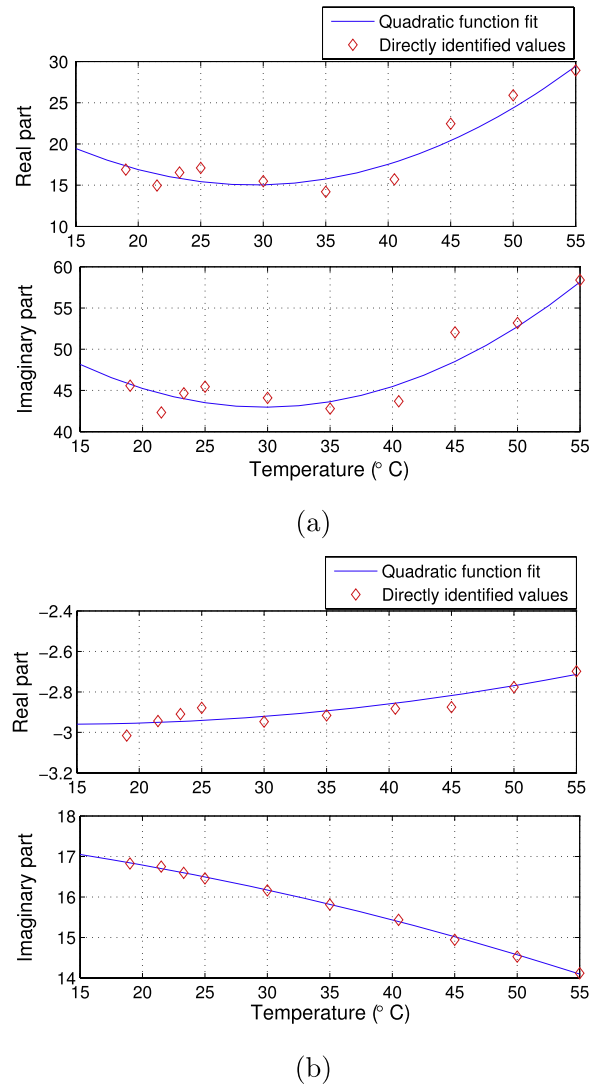


Figure 3. Approximation of temperature dependence of system parameters with quadratic functions: (a) zero z_1 and (b) pole p_1 . In each figure, the top and bottom plots show the real and imaginary components, respectively.

while using higher-degree polynomials could result in better fit between the experimental and predicted system parameters (zeros, poles and gain) at the tested temperatures, it is not necessarily desirable to do so. Because the empirically obtained parameters at a particular temperature have some inherent error from experimental uncertainties and model-fitting, matching minute details on the behaviors of these parameters does not always lead to improved predictive performance at other temperatures.

Using (3) with the gain, zeros and poles replaced with their temperature-dependent representations as illustrated in (4)–(9), we can obtain the model at any temperature in the experimental range. Figures 4(a) and (b) compare the temperature-dependent model-predicted frequency response with the measured frequency response at 35.0 °C and 45.0 °C, respectively. Note that the system models (also shown in figure 4 for comparison purposes) obtained by directly fitting the empirical response at 35.0 and 45.0 °C were not used

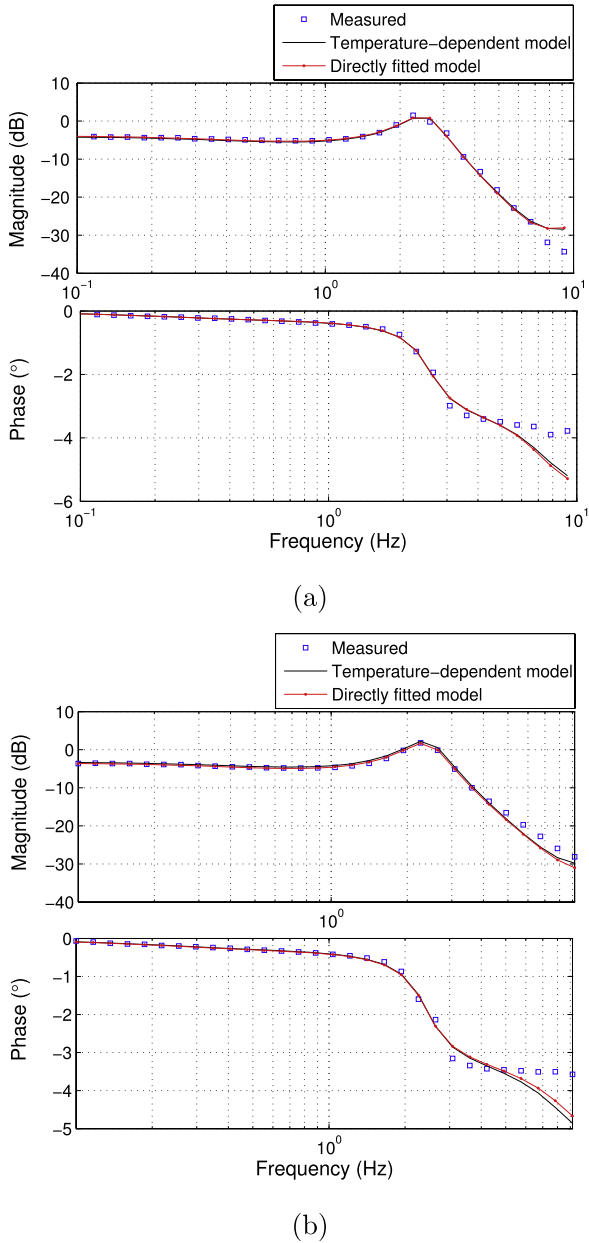


Figure 4. Comparison of the temperature-dependent model-based prediction with the measured frequency response and the directly fitted model-based prediction: (a) 35.0 °C and (b) 45.0 °C.

in deriving the temperature-dependent model. From figure 4, the temperature-dependent model provides an excellent approximation to the directly fitted model, and is capable of predicting the frequency response at new temperatures.

3. Inversion-based open-loop control

3.1. Inversion algorithm

In section 2.3 we have developed an approach to the modeling of temperature-dependent IPMC actuation dynamics. With an auxiliary measurement of the ambient temperature, one can then determine the current model and invert it to determine the open-loop control input.

Let $d(t)$ represent the tip displacement of the IPMC beam and let $v(t)$ represent the applied voltage to the IPMC, and let $D(s)$ and $V(s)$ represent their respective Laplace transforms. $V(s)$ and $D(s)$ are related with the temperature-dependent model $G_T(s)$:

$$D(s) = G_T(s)V(s). \quad (10)$$

Given a desired tip displacement trajectory $d(t)$, the open-loop control problem is to determine what voltage signal $v(t)$ needs to be applied to produce an output close to $d(t)$. Intuitively, this problem is solved with

$$V(s) = G_T^{-1}(s)D(s). \quad (11)$$

However, the model $G_T(s)$ is of non-minimum phase for any T in the operating range, which implies that $G_T^{-1}(s)$ is unstable and thus cannot be implemented. For example, from (6), the model at 35.0 °C has a pair of zeros located at $15.7416 \pm j43.6246$.

In this paper we explore the use of a stable but noncausal algorithm [58] to implement the inversion of $G_T(s)$. In principle, it requires knowing the full trajectory of the desired displacement in advance. While this assumption is restrictive and even unrealistic for certain applications, it is feasible for many other applications, especially applications involving repetitive motions of IPMC actuators, one example of which is an IPMC-actuated robotic fish [11]. In section 4, we will further discuss relaxing the assumption to requiring only a finite look-ahead time.

We will use a mixed Laplace and time-domain notation to facilitate the discussion, under which (10) is rewritten as

$$d(t) = G_T(s)[v](t), \quad (12)$$

where $G_T(s)[v]$ denotes the time-domain signal generated by passing $v(\cdot)$ through the system $G_T(s)$. If $H(s) = G_T(s)^{-1}$ were stable, the solution would be easily obtained by

$$v(t) = H(s)[d](t). \quad (13)$$

This approach, however, is infeasible since $H(s)$ has unstable poles. To proceed, we decompose $H(s) = H_s(s) + H_u(s)$, where $H_s(s)$ contains only the stable poles of $H(s)$ and $H_u(s)$ contains only the unstable poles of $H(s)$. Here we have assumed that $H(s)$ does not have any poles on the imaginary axis, or equivalently $G_T(s)$ does not have any pure imaginary zeros, which holds true for the obtained IPMC models. The specific forms of $H_s(s)$ and $H_u(s)$ for the IPMC case are

$$H_s(s) = \frac{1}{k} + \frac{r_3}{s - z_3}; \quad (14)$$

$$H_u(s) = \frac{r_1}{s - z_1} + \frac{r_2}{s - z_2}. \quad (15)$$

Figure 5 illustrates the proposed inversion algorithm. First, $d(t)$ is time-reversed to obtain $\tilde{d}(t) = d(-t)$, which is then passed through a stable system $\tilde{H}_u(s) \triangleq H_u(-s)$ to yield $\tilde{v}_u(t)$. The signal $\tilde{v}_u(t)$ is then time-reversed to produce $v_u(t)$. In parallel, the desired displacement signal $d(t)$ is run through $H_s(s)$ to generate $v_s(t)$. Recall $H(s) = H_s(s) + H_u(s)$. It follows that the final input to apply is $v(t) = v_s(t) + v_u(t)$.

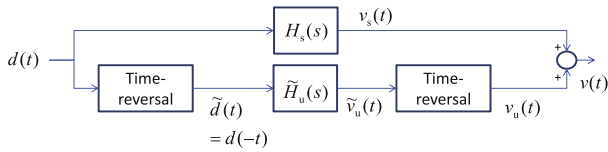


Figure 5. Schematic of the stable but noncausal inverse compensation algorithm.

3.2. Experimental results on open-loop tracking

We have conducted experiments to examine the effectiveness of the proposed open-loop control scheme. The IPMC was placed in the water bath with the temperature maintained at 45.0 °C. Three different desired trajectories for $d(t)$ were used: 0.5 Hz sinusoid, 2 Hz sinusoid and a combination of 0.5 and 2 Hz sinusoidal signals. For each of these desired trajectories, we implemented the inverse control scheme based on two different models, the model identified at $T = 19\text{ }^{\circ}\text{C}$ (scheme 1) and the temperature-dependent model with $T = 45.0\text{ }^{\circ}\text{C}$ (scheme 2).

Figures 6–8 show the experimental results. Overall the achieved displacement trajectories (especially those under scheme 2) follow well the desired ones, supporting that the inverse-based open-loop control strategy is effective. Furthermore, while the performance of scheme 2 is only slightly better than that of scheme 1 when tracking the 0.5 Hz signal (figure 6), its performance is significantly better when tracking the 2 Hz signal and the signal consisting of the sum of 0.5 and 2 Hz sinusoids (figures 7 and 8). Indeed, the bound on the tracking error under scheme 2 for the latter two cases is less than half of that under scheme 1. This can be explained by the effect of the temperature on the actuation behavior being much more pronounced at 2 Hz than at 0.5 Hz, as seen in figure 2. These results illustrate the importance of accommodating temperature-dependent dynamics in implementing the inverse control.

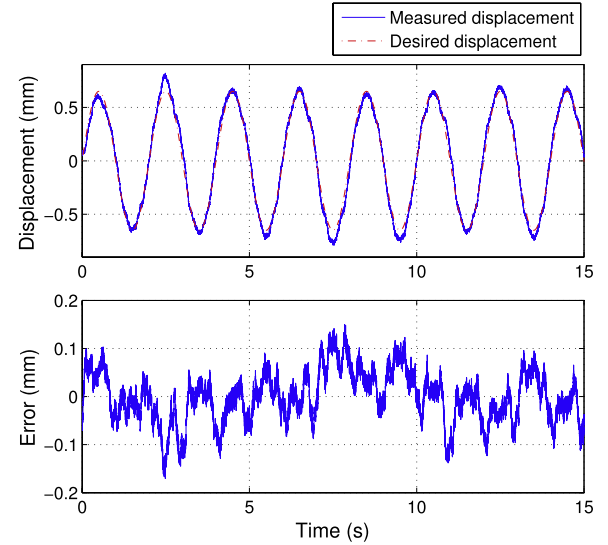
4. Inverse control with finite preview time

In principle, the inversion algorithm presented in section 3 requires knowing the desired output trajectory $d(\tau)$, $\forall \tau \geq t$ to compute the input value $v(t)$. In order to relax this assumption, here we briefly discuss the inversion algorithm with finite-time preview [59]. This algorithm requires knowing only $d(\tau)$, $\tau \in [t, t + T_p]$, for some finite $T_p > 0$, in order to evaluate $v(t)$. For the simplicity of discussion, we focus on the IPMC system that has been examined in section 3. To start, we note that

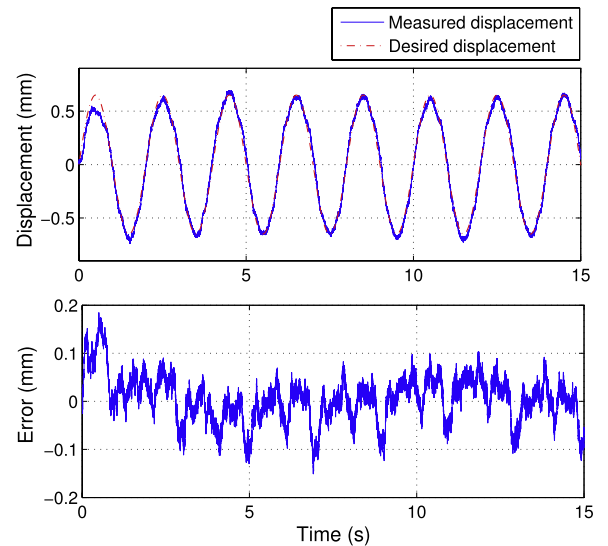
$$\begin{aligned} \tilde{H}_u(s) &= H_u(-s) = \frac{r_1}{-s - z_1} + \frac{r_2}{-s - z_2} \\ &= \frac{-r_1}{s + z_1} + \frac{-r_2}{s + z_2}, \end{aligned} \quad (16)$$

where z_1 and z_2 have strictly positive real parts, denoted as $r_0 > 0$. The impulse response of $\tilde{H}_u(s)$ is of the form

$$\tilde{h}_u(t) = -r_1 e^{-z_1 t} - r_2 e^{-z_2 t}, \quad (17)$$



(a)

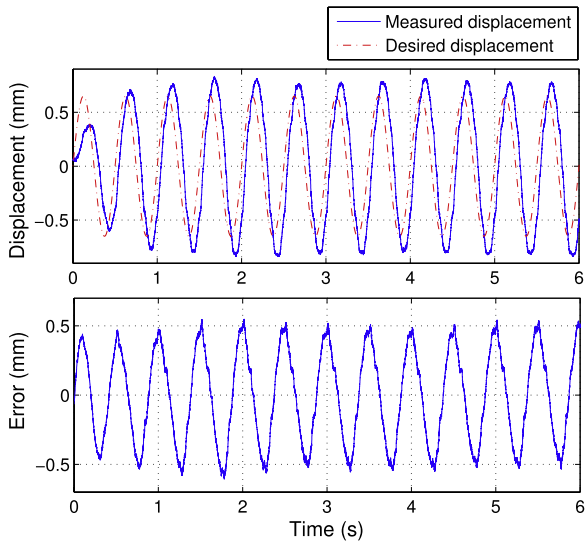


(b)

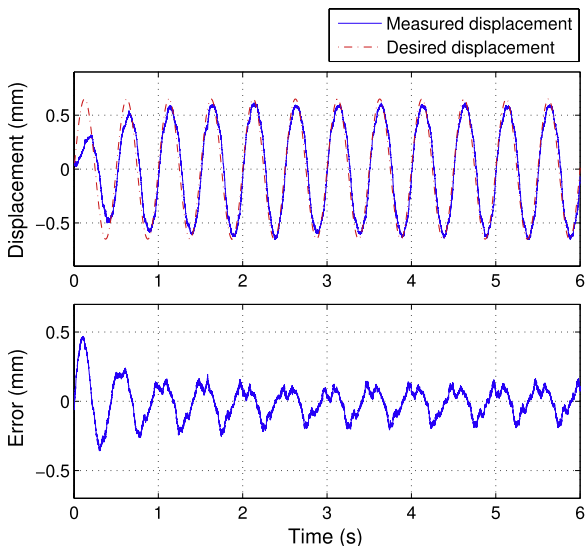
Figure 6. Experimental results on tracking a 0.5 Hz signal (amplitude 0.65 mm) with the bath temperature set at 45.0 °C: (a) Scheme 1 and (b) scheme 2. Scheme 1 is based on the inversion of the room-temperature model, while scheme 2 is based on the inversion of a model for 45.0 °C.

which approaches zero exponentially fast as t goes to ∞ , with the exponent determined by the real part r_0 of z_1 and z_2 . This implies that, for the system $\tilde{H}_u(s)$, its input prior to $t - T_0$ has negligible effect on its output at t , where T_0 depends on the time constant of $\tilde{H}_u(s)$, which can be represented as $\frac{1}{r_0}$. Equivalently, according to the inversion algorithm described in figure 5, the value of d beyond $t + T_0$ would have negligible impact on $v_u(t)$. The inversion algorithm with finite preview time thus works by treating the desired value of d beyond $t + T_0$ as zero, when evaluating $v_u(t)$.

We performed a simulation to illustrate this idea. For the IPMC model at $T = 45.0\text{ }^{\circ}\text{C}$, the value of r_0 was 20.41.



(a)



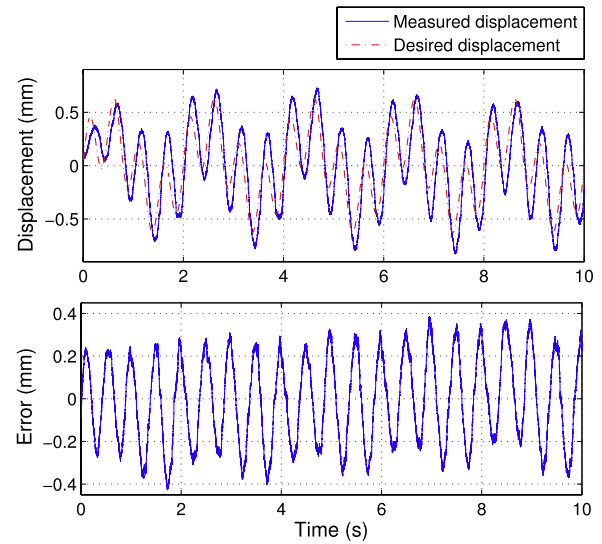
(b)

Figure 7. Experimental results on tracking a 2 Hz signal (amplitude 0.65 mm) with the bath temperature set at 45.0 °C: (a) scheme 1 and (b) scheme 2. Scheme 1 is based on the inversion of the room-temperature model, while scheme 2 is based on the inversion of a model for 45.0 °C.

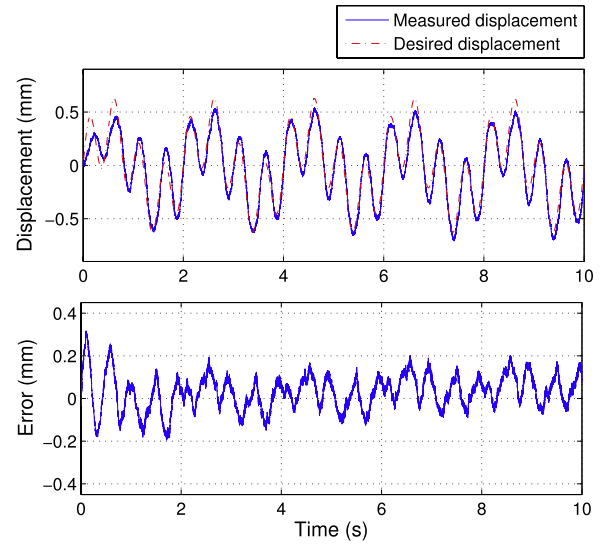
Figure 9 shows that, with a finite preview time of $\frac{6}{r_0}$, i.e. 0.294 s, the resulting displacement output provides good tracking of the desired trajectory. Considering the bandwidth of IPMC actuators (a few Hz), the required preview time is very feasible for most applications.

5. Conclusion

In this paper, we presented, to the best of our knowledge, the first study on control-oriented modeling of temperature-dependent actuation behavior of IPMCs. Furthermore, a stable but noncausal open-loop control scheme was proposed for



(a)



(b)

Figure 8. Experimental results on tracking a signal $0.325(\sin \pi t + \sin 4\pi t)$, with the bath temperature set at 45.0 °C: (a) scheme 1 and (b) scheme 2. Scheme 1 is based on the inversion of the room-temperature model, while scheme 2 is based on the inversion of a model for 45.0 °C.

an IPMC actuator subject to varying ambient temperatures, and the effectiveness of the scheme was supported by experimental results. A finite preview version of the algorithm was further discussed and illustrated with simulation results.

The proposed approach is empirical in nature. Therefore, the specific values of the model parameters, and even the functions describing the temperature dependence of the actuator behavior are of less relevance in general. What is important, however, is the general idea of how one might capture the temperature-dependent behavior based on the measurements at a few sampled temperatures and how such a model can be used for developing the open-loop controller.

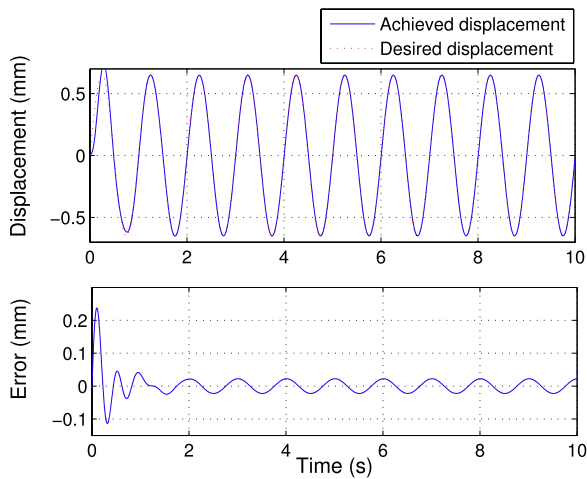


Figure 9. Simulation results on open-loop tracking control using inversion with a finite preview time of 0.294 s.

Such an approach can be readily extended to the modeling and control of other electroactive polymer materials [60] in the presence of thermal fluctuations.

There are several directions in which the present work can be extended. First, we note that there was still a noticeable tracking error even when a temperature-dependent model was used in the inversion; see figures 6–8. This was likely due to unmodeled nonlinearities and other time-varying factors in the IPMC actuator and its environment. For example, it is known that IPMCs demonstrate nonlinear dynamics [53, 54], so a linear model structure like the one used in the current paper can only capture the actuation behavior under a small applied voltage or around a particular operating point. Consequently, a model identified for a certain range of input amplitude may not work well for a different range. We also investigated the hysteresis effect associated with temperature changes; it was found that such hysteresis did exist, although its effect was not nearly as pronounced as the influence of the temperature itself. Refined modeling that takes into account these nonlinear effects is worthy of investigation and promises improved control performance. Second, since the temperature change appears to shift the resonant frequency of an IPMC actuator, as seen in figure 2, it is of interest to explore control schemes that adapt the operating frequency based on the temperature to maximize the actuation efficiency.

Acknowledgments

This research was supported in part by NSF (ECCS 0547131 and IIS 0916720) and ONR (grant N000140810640, program manager Dr T McKenna).

References

- [1] Shahinpoor M and Kim K 2001 Ionic polymer–metal composites: I. Fundamentals *Smart Mater. Struct.* **10** 819–33
- [2] Kim B, Ryu J, Jeong Y, Tak Y, Kim B and Park J-O 2003 A ciliary based 8-legged walking micro robot using cast

- IPMC actuators *Proc. IEEE Int. Conf. on Robots and Automation* pp 2940–5
- [3] Akle B, Bennett M and Leo D 2006 High-strain ionomeric–ionic liquid electroactive actuators *Sensors Actuators A* **126** 173–81
- [4] Chen Z and Tan X 2010 Monolithic fabrication of ionic polymer–metal composite actuators capable of complex deformation *Sensors Actuators A* **157** 246–57
- [5] Nemat-Nasser S and Li J 2000 Electromechanical response of ionic polymer–metal composites *J. Appl. Phys.* **87** 3321–31
- [6] Chen Z and Tan X 2008 A control-oriented and physics-based model for ionic polymer–metal composite actuators *IEEE/ASME Trans. Mech.* **13** 519–29
- [7] Farinholt K and Leo D 2004 Modeling of electromechanical charge sensing in ionic polymer transducers *Mech. Mater.* **36** 421–33
- [8] Chen Z, Tan X, Will A and Ziel C 2007 A dynamic model for ionic polymer–metal composite sensors *Smart Mater. Struct.* **16** 1477–88
- [9] Shahinpoor M and Kim K 2005 Ionic polymer–metal composites: IV. Industrial and medical applications *Smart Mater. Struct.* **14** 197–214
- [10] Takagi K, Yamamura M, Luo Z, Onish M, Hirano S, Asaka K and Hayakawa Y 2006 Development of a rajiform swimming robot using ionic polymer artificial muscles *Proc. 2006 IEEE/RSJ Int. Conf. on Intelligent Robots and Systems (Beijing)* pp 1861–6
- [11] Chen Z, Shatara S and Tan X 2010 Modeling of biomimetic robotic fish propelled by an ionic polymer–metal composite caudal fin *IEEE/ASME Trans. Mechatron.* **15** 448–59
- [12] Aureli M, Kopman V and Porfiri M 2010 Free-locomotion of underwater vehicles actuated by ionic polymer metal composites *IEEE/ASME Trans. Mechatron.* **15** 603–14
- [13] Yim W, Lee J and Kim K J 2007 An artificial muscle actuator for biomimetic underwater propulsors *Bioinsp. Biomim.* **2** S31–41
- [14] Brunetto P, Fortuna L, Graziani S and Strazzeri S 2008 A model of ionic polymer–metal composite actuators in underwater operations *Smart Mater. Struct.* **17** 025029
- [15] Kim K J, Pugal D and Leang K K 2011 A twistable ionic polymer–metal composite artificial muscle for marine applications *Mar. Technol. Soc. J.* **45** 83–98
- [16] Tan X 2011 Autonomous robotic fish as mobile sensor platforms: challenges and potential solutions *Mar. Technol. Soc. J.* **45** 31–40
- [17] Mojarad M and Shahinpoor M 1997 Ion-exchange-metal composite sensor films *Smart Structures and Materials 1997: Smart Sensing, Processing, and Instrumentation* vol 3042, ed R O Claus (Bellingham, WA: SPIE) pp 52–60
- [18] Ferrara L, Shahinpoor M, Kim K J, Schreyer H B, Keshavarzi A, Benzel E and Lantz J W 1999 Use of ionic polymer–metal composites (IPMCs) as a pressure transducer in the human spine *Smart Structures and Materials 1999: Electroactive Polymer Actuators and Devices* vol 3669, ed Y Bar-Cohen (Bellingham, WA: SPIE) pp 394–401
- [19] Keshavarzi A, Shahinpoor M, Kim K J and Lantz J W 1999 Blood pressure, pulse rate, and rhythm measurement using ionic polymer–metal composite sensors *Smart Structures and Materials 1999: Electroactive Polymer Actuators and Devices* vol 3669, ed J Bar-Cohen (Bellingham, WA: SPIE) pp 369–76
- [20] Konyo M, Konishi Y, Tadokoro S and Kishima T 2004 Development of velocity sensor using ionic polymer–metal composites *Smart Structures and Materials 2004: Electroactive Polymer Actuators and Devices* ed J Bar-Cohen (Bellingham, WA: SPIE) pp 307–18
- [21] Bonomo C, Fortuna L, Giannone P and Graziani S 2004 A sensor-actuator integrated system based on IPMCs [ionic

- polymer metal composites] *Proc. IEEE Sensors 2004* pp 489–92
- [22] Biddiss E and Chau T 2006 Electroactive polymeric sensors in hand prostheses: bending response of an ionic polymer metal composite *Med. Eng. Phys.* **28** 568–78
- [23] Bonomo C, Brunetto P, Fortuna L, Giannone P, Graziani S and Strazzeri S 2008 A tactile sensor for biomedical applications based on IPMCs *IEEE Sensors J.* **8** 1486–93
- [24] Ganley T, Hung D L, Zhu G and Tan X 2011 Modeling and inverse compensation of temperature-dependent ionic polymer–metal composite sensor dynamics *IEEE/ASME Trans. Mechatronics* **16** 80–9
- [25] Aureli M, Prince C, Porfiri M and Peterson S D 2010 Energy harvesting from base excitation of ionic polymer metal composites in fluid environments *Smart Mater. Struct.* **19** 015003
- [26] Bhat N D 2003 Modeling and precision control of ionic polymer metal composite *Master's Thesis* Texas A&M University
- [27] Richardson R C, Levesley M C, Brown M D, Hawkes J A, Watterson K and Walker P G 2003 Control of ionic polymer metal composites *IEEE/ASME Trans. Mechatronics* **8** 245–53
- [28] Yun K and jong Kim W 2006 Microscale position control of an electroactive polymer using an anti-windup scheme *Smart Mater. Struct.* **15** 924–30
- [29] Hunt A, Chen Z, Tan X and Kruusmaa M 2009 Feedback control of a coupled IPMC (ionic polymer–metal composite) sensor-actuator *Proc. ASME 2009 Dynamic Systems and Control Conf. (Hollywood, CA)* Paper DSCC2009–2700
- [30] Mallavarapu K and Leo D 2001 Feedback control of the bending response of ionic polymer actuators *J. Intell. Mater. Syst. Struct.* **12** 143–55
- [31] Kothera C S 2002 Micro-manipulation and bandwidth characterization of ionic polymer actuators *Master's Thesis* Virginia Polytechnic Institute and State University
- [32] Lavu B C, Schoen M P and Mahajan A 2005 Adaptive intelligent control of ionic polymer metal composites *Smart Mater. Struct.* **14** 466–74
- [33] Brufau-Penella J, Tsiakmakis K, Laopoulos T and Puig-Vidal M 2008 Model reference adaptive control for an ionic polymer metal composite in underwater applications *Smart Mater. Struct.* **17** 045020
- [34] Hao L and Li Z 2010 Modeling and adaptive inverse control of hysteresis and creep in ionic polymer metal composite actuators *Smart Mater. Struct.* **19** 025014
- [35] Punning A, Kruusmaa M and Aabloo A 2007 Surface resistance experiments with IPMC sensors and actuators *Sensors Actuators A* **133** 200–9
- [36] Punning A, Kruusmaa M and Aabloo A 2007 A self-sensing ion conducting polymer metal composite (IPMC) actuator *Sensors Actuators A* **136** 656–64
- [37] Kruusmaa K, Brunetto P, Graziani S, Punning A, Di Pasquale G and Aabloo A 2009 Self-sensing ionic polymer–metal composite actuating device with patterned surface electrodes *Polym. Int.* **59** 300–4
- [38] Newbury K M and Leo D J 2002 Electromechanical modeling and characterization of ionic polymer benders *J. Intell. Mater. Syst. Struct.* **13** 51–60
- [39] Yamakita M, Sera A, Kamamichi N, Asaka K and Luo Z W 2006 Integrated design of IPMC actuator/sensor *Proc. 2006 IEEE Int. Conf. on Robotics and Automation (Orlando, FL)* pp 1834–9
- [40] Hunt A, Chen Z, Tan X and Kruusmaa M 2010 Control of an inverted pendulum using an ionic polymer–metal composite actuator *Proc. 2010 IEEE/ASME Int. Conf. on Advanced Intelligent Mechatronics (Montreal)* pp 163–8
- [41] Song S, Shan Y, Kim K J and Leang K K 2010 Tracking control of oscillatory motion in IPMC actuators for underwater applications *Proc. 2010 IEEE/ASME Int. Conf. on Advanced Intelligent Mechatronics (Montreal)* pp 169–74
- [42] Chen Z, Shen Y, Xi N and Tan X 2007 Integrated sensing for ionic polymer–metal composite actuators using PVDF thin films *Smart Mater. Struct.* **16** S262–71
- [43] Chen Z, Kwon K and Tan X 2008 Integrated IPMC/PVDF sensory actuator and its validation in feedback control *Sensors Actuators A* **144** 231–41
- [44] Kanno R, Kurata A, Tadokoro S, Takamori T and Oguro K 1994 Characteristics and modeling of ICPF actuator *Proc. Japan–USA Symp. on Flexible Automation* pp 219–25
- [45] Kanno R, Tadokoro S, Takamori T and Hattori M 1996 Linear approximate dynamic model of IPMC (ionic conducting polymer gel film) actuator *Proc. IEEE Int. Conf. on Robotics and Automation (Minneapolis, MN)* pp 219–25
- [46] Newbury K M and Leo D J 2003 Linear electromechanical model for ionic polymer transducers—part I: model development *J. Intell. Mater. Syst. Struct.* **14** 333–42
- [47] Bonomo C, Fortuna L, Giannone P, Graziani S and Strazzeri S 2007 A nonlinear model for ionic polymer metal composites as actuators *Smart Mater. Struct.* **16** 1–12
- [48] de Gennes P G, Okumura K, Shahinpoor M and Kim K 2000 Mechanoelectric effects in ionic gels *Europhys. Lett.* **50** 513–8
- [49] Tadokoro S, Yamagami S, Takamori T and Oguro K 2000 Modeling of Nafion–Pt composite actuators (ICPF) by ionic motion *Smart Structures and Materials 2000: Electroactive Polymer Actuators and Devices; Proc. SPIE* **3987** 92–102
- [50] Farinholt K M 2005 Modeling and characterization of ionic polymer transducers for sensing and actuation *PhD Thesis* Virginia Polytechnic Institute and State University
- [51] Costa Branco P J and Dente J A 2006 Derivation of a continuum model and its electric equivalent-circuit representation for ionic polymer–metal composite (IPMC) electromechanics *Smart Mater. Struct.* **15** 378–92
- [52] Del Bufalo G, Placidi L and Porfiri M 2008 A mixture theory framework for modeling the mechanical actuation of ionic polymer metal composites *Smart Mater. Struct.* **17** 045010
- [53] Porfiri M 2008 Charge dynamics in ionic polymer metal composites *J. Appl. Phys.* **104** 104915
- [54] Chen Z, Hedgepeth D R and Tan X 2009 A nonlinear, control-oriented model for ionic polymer–metal composite actuators *Smart Mater. Struct.* **18** 055008
- [55] Pugal D, Kim K J and Aabloo A 2010 Modeling the transduction of IPMC in 3D configurations *Behavior and Mechanics of Multifunctional Materials and Composites; Proc. SPIE* **7644** 76441T
- [56] Zangrilli U and Weiland L M 2011 Prediction of the ionic polymer transducer sensing of shear loading *Smart Mater. Struct.* **20** 094013
- [57] Ganley T, Hung D L, Zhu G and Tan X 2011 Modeling and inverse compensation of temperature-dependent ionic polymer–metal composite sensor dynamics *IEEE/ASME Trans. Mechatronics* **16** 80–9
- [58] Devasia S, Chen D and Paden B 1996 Nonlinear inversion-based output tracking *IEEE Trans. Autom. Control* **41** 930–42
- [59] Zou Q and Devasia S 2004 Preview-based optimal inversion for output tracking: application to scanning tunneling microscopy *IEEE Trans. Control Syst. Technol.* **12** 375–86
- [60] Fang Y, Tan X and Alici G 2008 Robust adaptive control of conjugated polymer actuators *IEEE Trans. Control Syst. Technol.* **16** 600–12